

## Chapter 22

### An Energy Recovery Linac for the LHC

S. Alex Bogacz, Bernhard J. Holzer and John A. Osborne

*European Organization for Nuclear Research (CERN),  
Genève, Switzerland*

*Center for Advanced Studies of Accelerators, Jefferson Lab (TJNAF),  
Newport News, USA*

The LHeC provides an intense, high energy electron beam to collide with the LHC as the sole opportunity for a next energy frontier electron-hadron collider. It represents the highest energy application of energy recovery linac (ERL) technology — which is increasingly recognised as one of the major pilot technologies for the development of particle physics because it utilises and stimulates superconducting RF technology progress, and it increases intensity while keeping the power consumption low. The LHeC instantaneous luminosity is determined through the integrated luminosity goal. The electron beam energy is chosen to achieve TeV cms collision energies and enable competitive searches and precision Higgs boson measurements. The wall-plug power has been constrained to about 100 MW. Two super-conducting linacs of about 900 m length, which are placed opposite to each other, accelerate the passing electrons by 8.3 GeV each. This leads to a final electron beam energy of about 50 GeV in a 3-turn racetrack energy recovery linac configuration.

#### 1. Introduction

Within half a century, particle physics has established a Standard Model (SM) for the description of the fundamental constituents of matter and their electroweak and strong interactions. Besides confirming the SM in many (previously unexplored) areas, the largest contribution of the LHC to the development of particle physics, so far, has been the discovery of the

---

This is an open access article published by World Scientific Publishing Company. It is distributed under the terms of the [Creative Commons Attribution 4.0 \(CC BY\) License](https://creativecommons.org/licenses/by/4.0/).

Higgs boson and the study of its properties. The Standard Model, however, despite its phenomenological success, has severe deficiencies. For example, it lacks the “grand unification” of the particle interactions, has more than twenty free parameters, does not explain the existence of 3 quark and lepton families nor the difference between the nature of leptons and quarks. The strong interaction in the SM is described by Quantum Chromodynamics (QCD), which is still far from being completely developed, e.g., neither has it provided an explanation of parton confinement — a prediction about which substructure layers may exist, nor have its assumptions on non-linear dynamics in high parton density regimes been verified.

In the past decades of research on elementary particle physics, progress has been made with a threefold strategy by exploring each level of high energy with hadron-hadron, electron-positron and lepton-hadron experiments mostly based on colliders. This holds for the beginning and later for the time of the exploration of nature with the Sp $\bar{p}$ S, PETRA/PEP and the fixed target electron, neutrino and muon-hadron experiments. It was repeated when the Tevatron, LEP/SLC and HERA accessed the Fermi energy scale corresponding to the masses of the weakly interacting bosons,  $Z$  and  $W^\pm$ , and the top quark.

With the LHC a new era began, that of exploring the SM at even higher energies and searching for its possible extensions in the TeV energy range. A new electron-positron collider has been proposed to be built, with several candidate technologies for a new enlarged ring machine (FCC-ee at CERN and CEPC in China) or based on linear collider techniques (ILC, CLIC, or more recent concepts using high gradient or energy recovery variations). For a next generation lepton-hadron collider extending the energy frontier into the TeV region, the hadron (proton and ion) beams of the LHC provide the only realistic foundation for the coming decades. This has been recognised with the accelerator, physics and detector developments of the Large Hadron Electron Collider (LHeC), as has been documented in an initial, detailed, refereed Conceptual Design Report which was published in 2012,<sup>1</sup> at the time of the discovery of the Higgs Boson. A similarly detailed report<sup>2</sup> on the LHeC appeared in 2020, accounting for a decade of further developments of physics as well as accelerator and detector technologies.

This work, undertaken by hundreds of contributing physicists and engineers, mandated by CERN and ECFA, has provided a novel electron-hadron collider design with a few salient characteristics: i) the combination of the LHC proton beam with an about 50 GeV, 3-turn, intense energy recovery racetrack-linac accelerator resulted in a realistic, affordable design

exceeding the parameters of HERA by a factor of twenty in kinematics and nearly 1000 in luminosity; ii) the LHeC design is for concurrent LHC and LHeC operation which, conceptually, does not reduce the LHC running time; iii) owing to the  $10^{34} \text{ cm}^{-2}\text{s}^{-1}$  achievable instantaneous luminosity, the LHeC has a competitive Higgs physics and BSM search potential while providing ample luminosity for unprecedented research in the strong and electroweak interaction area<sup>2</sup> as is summarised in subsequent sections of this book; iv) the introduction of energy recovery technology stands out as an example for the required low power requests to the next generation of colliders for particle physics.

Each significant step of beam energy increase has provided deeper, often unexpected insights to the characteristics of elementary particle physics. With lepton-hadron experiments, a series of discoveries were made: of the finite proton size; of the existence of parton substructure and the confirmation of the quark-parton model; with the proof for the electron to weakly couple as a right-handed singlet, the decisive verification of the Glashow-Weinberg-Salam theory in 1978; later with the first measurements on parton momentum distributions and the discovery of high gluon and sea-quark densities and deep inelastic diffraction. There is hardly a quantitative understanding of the LHC pp interactions without the HERA input. The LHeC can be expected to unravel further surprises, while leading to a much deeper understanding of parton dynamics and the Higgs mechanism, and through that of LHC physics.

In order for a combined hh and eh ( $h = p, A$ ) collider configuration to become a realistic, attractive scenario all essential aspects of the novel electron ERL, the main component of the LHeC, had to be carefully studied.<sup>1,2</sup> The following sections present an overview on the LHeC (Sec. 2) and three particularly challenging developments: the design of an optimum lattice for a 3-turn electron beam using two linacs opposite to each other in the straight sections (Sec. 2.1), the layout of an interaction region able to deal with the colliding electron and hadron beams while letting the non-colliding hadron beam pass (Sec. 2.2) and, finally, a study of the civil engineering aspects of placing a racetrack tunnel of about 6 km circumference in the vicinity of the LHC ring for enabling electron-hadron interactions (Sec. 2.3). Further sections provide overviews on various key aspects of physics at the LHeC and a design concept for a novel detector to deliver electron-proton and -ion physics in the new ranges of energy and luminosity.

The LHeC design has been adopted for the initial layout of the 3.5 TeV cms energy electron-hadron facility at the Future Circular Collider

(FCC-eh<sup>3</sup>). Should the LHeC be built, its key accelerator parts are considered to be relocatable to the FCC. If the LHC would be upgraded in energy, the investment in the LHeC would even more directly pay off as the electron accelerator could promptly be used for deep inelastic scattering (DIS) physics at even higher energy and intensity, at the HE-LHC. Furthermore, the electron accelerator of the LHeC may be used as the injector of a future FCC-ee machine allowing direct top-up injection at W production energies.

## 2. The ERL Configuration of the LHeC

The LHeC provides an intense, high energy electron beam to collide with the LHC. Furthermore, it pushes energy recovery linac (ERL) technology into an unprecedented beam energy regime, which is increasingly recognised as one of the major pilot technologies for the development of particle physics. Finally, it utilises and stimulates superconducting RF technology progress, and it increases intensity while keeping the power consumption manageable. The electron beam energy is chosen to achieve TeV cms collision energy and enable competitive searches and precision Higgs boson measurements. A cost-physics-energy evaluation, presented in Ref. 4, points to choosing  $E_e \simeq 50$  GeV as a new default value, which was 60 GeV before. The wall-plug power has been constrained to 140 MW. The main parameters of the LHeC ERL are listed in Table 1.

Table 1. Parameters of LHeC Energy Recovery Linac (ERL).

Parameter	Unit	Value
Injector energy	GeV	0.5
Maximum electron energy	GeV	49.19
Bunch charge	pC	499
Bunch spacing	ns	24.95
Electron current	mA	20
Total energy gain per linac	GeV	8.114
Frequency	MHz	801.58
Acceleration gradient	MV/m	19.73
Number of cells per cavity		5
Cavities per cryomodule		4
Cryomodule length	m	7
Total ERL length	km	5.332

The ERL consists of two superconducting (SC) linacs operated in CW connected by at least three pairs of arcs to allow three accelerating and

three decelerating passes (see Fig. 1). The length of the high energy return arc following the interaction point should be able to provide a half RF period wavelength shift to allow the deceleration of the beam in the linac structures in three passes down to the injection energy and its safe disposal. SC Cavities with an unloaded quality factor  $Q_0$  exceeding  $10^{10}$  are required to minimise the requirements on the cryogenic cooling power and to allow an efficient ERL operation. The choice of having three accelerating and three decelerating passes implies that the circulating current in the linacs is six times the current colliding at the Interaction Point (IP) with the hadron beam.

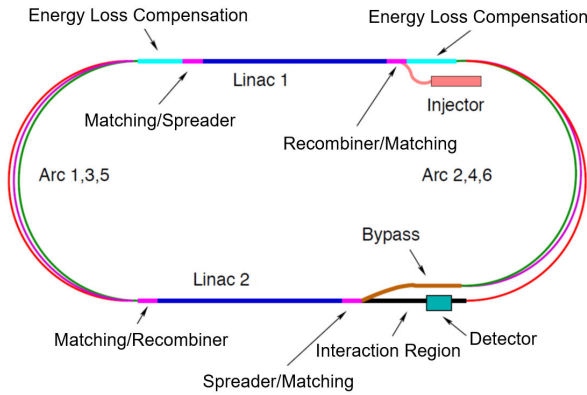


Fig. 1. Schematic layout of the LHeC design based on an Energy Recovery Linac.

## 2.1. Linac Configuration and Multi-pass Optics

Appropriate choice of the linac optics is of paramount importance for the transverse beam dynamics in a multi-pass ERL. The focusing profile along the linac (quadrupole gradients) needs to be set (and they stay constant), so that multiple pass beams within a vast energy range may be transported efficiently. The chosen arrangement is such that adequate transverse focusing is provided for a given linac aperture. The linac optics is configured as a strongly focusing,  $130^0$  FODO. In a basic FODO cell a quadrupole is placed every four cryomodules, so that the full cell contains two groups of 16 RF cavities and a pair of quads (F, D). Energy recovery in a racetrack topology explicitly requires that both the accelerating and decelerating beams share the individual return arcs.<sup>5</sup> This, in turn, imposes specific requirements for

TWISS function at the linacs ends: TWISS functions have to be identical for both the accelerating and decelerating linac passes converging to the same energy and therefore entering the same arc.

As extensively discussed in Ref. 6, the corresponding accelerating and decelerating passes are joined together at the arc's entrance/exit. The optics of the two linacs are mirror-symmetric; They were optimised such that, Linac 1 is periodic for the first accelerating pass and Linac 2 has this feature for last decelerating one. In order to maximize the BBU (Beam Breakup) Instability threshold current,<sup>7</sup> the optics is tuned so that the integral of  $\beta/E$  ( $\beta$  being the betatron function and  $E$ , beam energy) along the linac is minimised.

### 2.1.1. *Spreaders and Recombiners*

The spreaders are placed directly after each linac to separate beams of different energies and to route them to the corresponding arcs. The recombiners facilitate just the opposite: merging the beams of different energies into the same trajectory before entering the next linac. Each spreader starts with a vertical bending magnet, common for all three beams, that initiates the separation. The highest energy, at the bottom, is brought back to the horizontal plane with a chicane. The lower energies are captured with a two-step vertical bending adapted from the CEBAF design.<sup>8</sup> The vertical dispersion is suppressed by a pair of quadrupoles located in-between vertical steps. An alternative spreader design with a single vertical step has been explored as well. That option was not retained due to the superconducting technology needed for the quadrupoles that must be avoided in this highly radiative section.

### 2.1.2. *Synchrotron Radiation — Emittance Preserving Optics*

Synchrotron radiation effects on beam dynamics, such as the energy loss, as well as the transverse and longitudinal emittance dilution induced by quantum excitations, have a paramount impact on the collider luminosity. These quantities, first introduced by M. Sands<sup>9</sup> are summarized below:

$$\Delta E = \frac{2\pi}{3} r_0 mc^2 \frac{\gamma^4}{\rho} \quad (1)$$

$$\Delta \epsilon_N = \frac{2\pi}{3} C_q r_0 \langle H \rangle \frac{\gamma^6}{\rho^2}, \quad (2)$$

$$\frac{\Delta\epsilon_E^2}{E^2} = \frac{2\pi}{3} C_q r_0 \frac{\gamma^5}{\rho^2}, \tag{3}$$

where  $C_q = \frac{55}{32\sqrt{3}} \frac{\hbar}{mc}$ . Here,  $\Delta\epsilon_E^2$  is an increment of energy square variance,  $r_0$  is the classical electron radius,  $\gamma$  is the Lorentz boost and  $C_q \approx 3.832 \cdot 10^{-13}$  m for electrons (or positrons). Here,  $H = (1 + \alpha^2)/\beta \cdot D^2 + 2\alpha DD' + \beta \cdot D'^2$  where  $D, D'$  are the bending plane dispersion and its derivative, with  $\langle \dots \rangle = \frac{1}{\pi} \int_{\text{bends}} \dots d\theta$ .

Therefore, emittance dilution can be mitigated through appropriate choice of arc optics (values of  $\alpha, \beta, D, D'$  at the bends). In the presented design, the arcs are configured with a FMC (Flexible Momentum Compaction) optics to ease individual adjustment of emittance dispersion averages,  $\langle H \rangle$ , in various energy arcs.

Optics design of each arc takes into account the impact of synchrotron radiation at different energies. At the highest energy, it is crucial to minimise the emittance dilution due to quantum excitations; therefore, the cells are tuned to minimise the emittance dispersion,  $H$ , in the bending sections, as in the TME (Theoretical Minimum Emittance) lattice. The higher energy arcs (4, 5 and 6) configured with the TME cells still quasi-isochronous. All styles of FMC lattice cells, as illustrated in Fig. 2, share the same footprint for each arc. This allows us to stack magnets on top of each other or to combine them in a single design.

Cumulative dilution of the transverse,  $\Delta\epsilon_N$ , and longitudinal,  $\Delta\sigma_{\frac{\Delta E}{E}}$ , emittance due to quantum excitations calculated using analytic formulas,

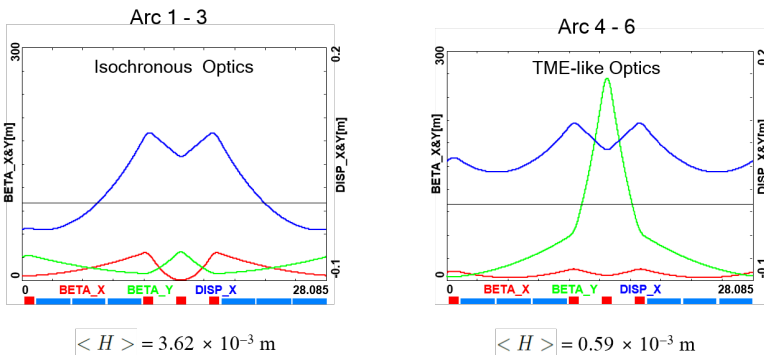


Fig. 2. Two styles of FMC cells appropriate for different energy ranges. Left: lower energy arcs (Arc 1–3) configured with *Isochronous* cells, Right: higher energy arcs configured with *TME-like* cells. Corresponding values of the emittance dispersion averages,  $\langle H \rangle$ , are listed for both style cells.

Eqs. (1), (2) and (3), at the end of arc 6 (including spreaders, recombiners and pathlength correcting 'doglegs') can be summarized as follows:<sup>2</sup> about 25 mm mrad (in both the horizontal and vertical plane) and 0.24%. Net energy loss of 836 MeV has to be replenished back to the beam, so that at the entrance of each arc the accelerated and decelerated beams have the same energy, unless separate arcs are used for the accelerated and decelerated beams. As discussed in detail in Ref. 6, the compensation makes use of a second harmonic RF at 1603.2 MHz to replenish the energy loss for both the accelerated and the decelerated beams.

## 2.2. Interaction Region

The Interaction Region (IR) of the ERL is one of the most challenging parts of the machine: While seeking for highest luminosity in ep-collisions, the bunches have to be separated after collision and guided to their lattice structures, to avoid parasitic bunch encounters. In addition, beam-beam effects with the second non-colliding proton beam have to be avoided. In order to meet these requirements, the design of the IR has been based on a compact magnet structure for an effective beam separation and smallest synchrotron radiation effects in the Interaction Region (IR). Following the design of the LHC upgrade project, HL-LHC, and the layout of the ERL for the electrons, the parameter list of the LHeC has been defined, Table 2, leading to a luminosity at the e-p interaction point in the order of  $L = 10^{34} \text{ cm}^{-2}\text{s}^{-1}$ .

Table 2. Parameter list of the LHeC.

Parameter	Unit	Electrons	Protons
beam energy	GeV	50	7000
beam current	mA	20	1400
bunches per beam	-	1188	2808
bunch population	$10^{10}$	0.3	22
bunch charge	nC	0.5	35.24
norm. emittance (at IP)	mm · mrad	30	2.5
beta function at IP	cm	10.9	10
beam-beam disruption	-	14.3	$1 \cdot 10^{-5}$
luminosity	$\text{cm}^{-2}\text{s}^{-1}$	$0.7 \cdot 10^{34}$	



### 2.2.1. Electron Beam Optics and Separation Scheme

A manifold of conditions are taken into account: Focusing of the electron beam to the required  $\beta$  values in both planes, sufficient beam separation, optimisation of the beam separation for smallest critical energy and synchrotron light power, and sufficient space for the detector hardware. A separation scheme has been established<sup>10</sup> that combines these requirements in one lattice structure (Fig. 3). Due to the different rigidity of the beams, a separation is possible by applying a series of magnets, acting as quasi-constant deflecting field: The spectrometer dipole of the LHeC detector ( $B0$ ) is used to establish a first separation. Right after and as close as possible to the IP, the mini-beta quadrupoles of the electron beam are located. A doublet design allows highest compactness of the IR layout and provides focusing in both planes for matched beam sizes of protons and electrons at the IP,  $\beta_x(p) = \beta_x(e)$ ,  $\beta_y(p) = \beta_y(e)$ . The two quadrupoles are positioned off-center with respect to the electron beam, acting as combined function magnets to provide a continuous soft bending of the electron beam throughout the complete magnet structure.

As indicated in (Fig. 3) the co-action of an early focusing scheme of electrons, the use of off-centre quadrupoles and the minimised beam size at the separation point lead to a considerable reduction of critical energy and power of the emitted light. The presently obtained values of 250 keV and 19 kW respectively are still challenging and considered as work in progress. Especially in the context of the HL-LHC luminosity upgrade the free space available for beam separation will increase, leading to a further reduction of the synchrotron light parameters.

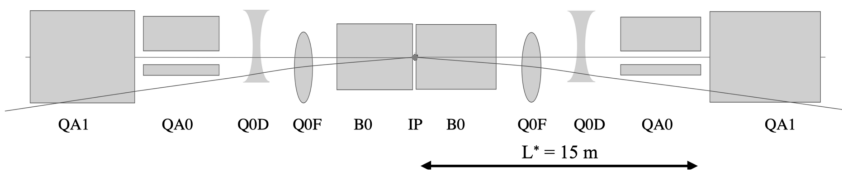


Fig. 3. Schematic view of the combined focusing - beam separation scheme.

### 2.2.2. Proton Beam Optics

The optics of the colliding proton beam follows the standard settings of the HL-LHC and is based on the so-called ATS scheme (achromatic telescoping

squeeze). It allows smaller values of  $\beta^*$  at a given collision point — and thus higher luminosity. Figure 4 shows the proton optics for values of e.g.  $\beta^* = 7$  cm at the interaction point of the LHeC — embedded and well matched into the HL-LHC optics for the ATLAS and CMS interaction points. The long-ranging beta-beat, which is an essential feature of the HL-LHC optics,<sup>11</sup> is clearly visible on both sides of the IP.

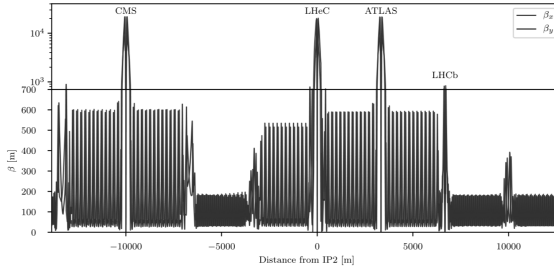


Fig. 4. LHC proton beam optics, optimised for values of  $\beta = 7$  cm at the LHeC IP.

The operation of the LHeC electron-proton collisions is foreseen in parallel to the LHC standard p-p operation. As a consequence, the design orbit of the second “non-colliding” proton beam at the e-p interaction point must be included in the e-p IR layout. At the e-p interaction region, a collision of the two proton beams is avoided by selecting appropriately its location: Shifted in position and thus in time, direct collisions between the two proton beams as well as with the electron beam can be excluded. All in all the e-p interaction region, including the mini-beta structure of the electron beam, is embedded in the existing LHC lattice to allow for concurrent e-p and p-p collisions in the LHC interaction points.

### 2.2.3. Beam-Beam Effects

The beam-beam effect will always be a strong limitation of a particle collider and care has to be taken, to preserve the beam quality of proton and electron beam. In case of the proton beam, the beam beam effect has to be limited to preserve the proton beam emittance and allow successful parallel data taking in the p-p collision points. Due to the limited bunch population of the electron beam, this is fulfilled by design. In the case of the electron beam the beam-beam effect is determined by the proton bunch population, which is considerably higher than the electron bunch intensity and its detrimental effects on the electron emittance had to be limited to assure

a successful energy recovery process in the ERL. As was comprehensively simulated in Ref. 10, the core of the beam still remains in a quasi ellipse like boundary, while tails in the transverse beam distribution are clearly visible (as consequence of the beam-beam effect). The simulation showed that these tails are still compatible with the energy recovery process.

## 2.3. Civil Engineering

### 2.3.1. Introduction

Since the beginning of the LHeC concept, various shapes and sizes of the eh collider were studied around CERN region. The conceptual study report published in 2012 focused primarily on two main options, namely the RING-RING and the LINAC-RING options. For civil engineering, these options were studied, taking into account geology, construction risks, land features as well as technical constrains and operation of the LHC. The Linac-Ring configuration was chosen as baseline for its largely decoupled CE and installation work from the nominal LHC operation.

This chapter describes the civil engineering infrastructure required for an Energy Recovery Linac (ERL) injecting into the LHC ALICE cavern at LHC Point 2. Figure 5 shows three options of different sizes proposed for the ERL, represented as fractions of the LHC circumference. This chapter focuses on the currently preferred option, specifically the 1/5 of the LHC circumference.

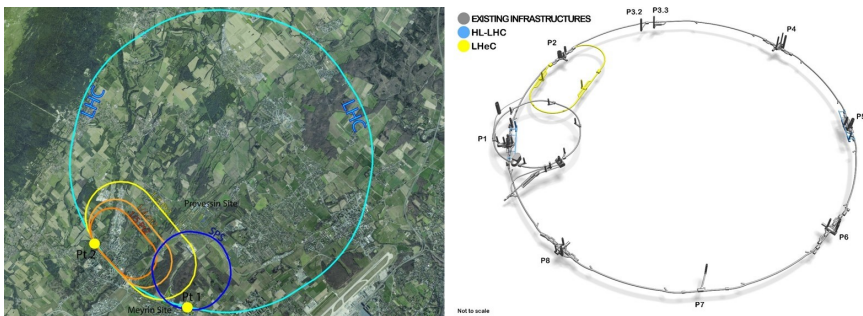


Fig. 5. Three racetrack alternatives proposed for the eh machine at LHC Point 2 (left) and 3D schematic showing the proposed racetrack of the Large Hadron electron Collider at high luminosity (right).

### 2.3.2. Placement and Geology

The proposed site for the LHeC is in the North-Western part of the Geneva region at the existing CERN laboratory. The proposed Interaction Region is fully located within existing CERN land at LHC Point 2, close to the village of St. Genis, in France. The CERN area is extremely well suited to housing such a large project, with well understood ground conditions having several particle accelerators in the region for over 50 years. Extensive geological records exist from previous projects such as SPS, LEP and LHC and more recently, further ground investigations have been undertaken for the High-Luminosity LHC project. Any new underground structures will be constructed in the stable molasse rock at a depth of 100–150 m in an area with very low seismic activity.

The ERL will be positioned inside the LHC Ring, in order to ensure that new surface facilities are located on existing CERN land. The proposed underground structures for a Large Hadron electron Collider (LHeC) at high luminosity aiming for an electron beam energy of 50 GeV is shown in Fig. 5. The LHeC tunnel will be tilted similarly to the LHC at a slope of 1.4% to follow a suitable layer of molasse rock.

### 2.3.3. Underground infrastructure

The underground structures proposed for LHeC in the proposed design with a  $1/5$  LHC circumference require a tunnel approximately 5.4 km long of 5.5 m diameter, including two LINACs. Parallel to the main LINAC tunnels, at 10 m distance apart, are the RF galleries, each 830 m long. Waveguides of 1 m diameter are connecting the RF galleries and LHeC main tunnel.

Two additional caverns, 25 m wide and 50 m long are required for cryogenics and technical services. These are connected to the surface via two 9 m diameter access, provided with lifts to allow access for equipment and personnel. Additional caverns are needed to house injection facilities and a beam dump.

In addition to the new structures, the existing LHC infrastructure also requires modifications. To ensure connection between LHC and LHeC tunnels, the junction caverns UJ22 and UJ27 need to be enlarged. Localised parts of the cavern and tunnel lining will be broken out to facilitate the excavation of the new spaces and the new connections, requiring temporary support.

Infrastructure works for LEP were completed in 1989, for which a design

lifespan of 50 years was specified. If LHC is to be upgraded with a high energy, refurbishment, maintenance works are needed to re-use the existing infrastructure. Shaft locations were chosen such that the surface facilities are located on CERN land. The scope for surface sites is still to be defined. New facilities are envisaged for housing technical services such as cooling and ventilation, cryogenics and electrical distribution.

#### 2.3.4. Construction Methods

A Tunnel Boring Machines (TBM) should be utilised for the excavation of the main tunnel to achieve the fastest construction. When ground conditions are good and the geology is consistent, TBMs can be two to four times faster than conventional methods. A shielded TBM could be employed, with pre-cast segmental lining, and injection grouting behind the lining.

For the excavation of the shafts, caverns and connection tunnels, conventional technique could be used. Similar construction methods as for HL-LHC, for example using roadheaders and rockbreakers, can be adopted for LHeC. Some of these machinery can be seen in Fig. 6, showing the excavation works at point 1 HL-LHC. One main constraint that dictated the equipment used for the HL-LHC excavation was the vibration limit. Considering the sensitivity of the beamline, diesel excavators have been modified and equipped with an electric motor in order to reduce vibrations that could disrupt LHC operation. A similar equipment could also be needed for LHeC if construction works are carried out during operation of the LHC.



Fig. 6. Excavator with hydraulic cutting heads being used at HL-LHC Point 1.

Existing boreholes data around IP2 shows that the moraines layer can be 25–35 m deep before reaching the molasse. Temporary support of the excavation, for example using diaphragm walls, are recommended. Once reaching a stable ground in dry conditions, common excavation methods can be adopted, for example using roadheaders and rockbreakers. The shaft lining will consist of a primary layer of shotcrete with rockbolts and an in-situ reinforced concrete secondary lining, with a waterproofing membrane in between the two linings.

### 2.3.5. Cost Estimate

A cost estimate was prepared for a 9.1 km ERL located at Point 2 of LHC, using the same measure prices as for FCC. More recently for LHeC, the cost figures were adapted to fit the smaller version, the 5.4 km racetrack at Point 2 (option 1/5 LHC).

The civil engineering costs amount to about 25% of the total project costs. In particular, for a 9.1 km ERL (1/3 LHC option) the civil engineering was estimated to 386 MCHF and for a 5.4 km configuration (1/5 LHC) the costs is 289 MCHF. These estimates include the fees for preliminary design, approvals and tender documents (12%), site investigations (2%) and contractor's profit (3%). The costs mentioned do not include surface structures. Where possible, existing surface infrastructure will be re-used.

## 3. Outlook

### 3.1. The ERL Development Facility PERLE at Orsay

PERLE (Powerful ERL for Experiments)<sup>2,12</sup> — a 'stepping stone' to the LHeC — is envisioned as a novel ERL test facility, designed to validate choices for a high energy ERL foreseen in the design of the Large Hadron electron Collider (50 GeV) and the Future Circular Collider (FCC-eh, 60 GeV). PERLE is a compact ERL, resembling the LHeC configuration, based on superconducting RF technology, expands the operational regime for ERLs to 10 MW of beam power. This is achieved with 20 mA electron current, as foreseen for the LHeC, and 500 MeV electron beam energy generated in 3 passes through two linac modules. The cryomodules equipped with four 5-cell Niobium cavities, and other elements of PERLE may directly be applied to future, more complex accelerators. One may envision PERLE being used as the injector for the LHeC. PERLE is being built at the IJC Laboratory at Orsay near Paris by an International Collaboration.

The facility was described and recognized in 2021 as a key part of the European Roadmap towards novel accelerators<sup>13</sup> for its unique characteristics paving the way not only for sustainable, multi-turn ERL technology, but also for pioneering industrial and low energy physics applications.

### 3.2. *The Future of the LHeC*

The Large Hadron electron Collider has been designed<sup>2</sup> as a novel part of the LHC facility with a far reaching physics program — both for energy frontier deep inelastic electron-hadron scattering and for empowering the exploration of proton-proton and heavy ion physics at the LHC. It builds on the complex, existing, expensive infrastructure of the LHC and represents the most economic way towards a higher precision Higgs physics program, which specifically relies on energy recovery technology at high currents. ERL is a principal means for reducing the power consumption for the next generation of lepton colliders. Operating without energy recovery, the LHeC would use GWs of power. Thanks to employing the energy recovery, the net power is reduced to 100 MW or possibly even lower. It thus is a first large scale example of an energy efficient particle physics accelerator, for which PERLE primarily provides and tests the required technology.

The book on the future of the LHC is being written, for the time beginning with and yet reaching beyond its high luminosity phase. The physics at the Fermi scale was explored about two decades ago with the hadron collider Tevatron, the  $e^+e^-$  collider LEP and the first ep collider HERA. The LHeC represents the unique and timely possibility to accompany the hadron collider LHC with a partner electron-hadron collider to gain the necessary insight for particle physics to proceed. The Standard Model may then possibly be included in a fundamental theory of particles and their interactions. These developments cannot proceed without a next generation of energy frontier colliders, including one for TeV energy deep inelastic scattering. The LHeC can be realised with the HL-LHC and it may come with the HE-LHC. Its visionary prospect is the 3.5 TeV version, the FCC-eh.

### Funding Information

Work at Jefferson Lab has been supported by the U.S. Department of Energy, Office of Science, Office of Nuclear Physics under contracts DE-AC05-06OR23177 and DE-SC0012704.

## Acknowledgments

Useful discussions and conceptual input from: Kevin André, Oliver Brüning, Max Klein, Walid Kaabi, Dario Pellegrini and Alessandra Valloni at all stages of the accelerator design process are greatly acknowledged.

## References

1. J. L. Abelleira et al., A Large Hadron Electron Collider at CERN: Report on the Physics and Design Concepts for Machine and Detector, *J. Phys.* **G39**, 075001 (2012). doi: 10.1088/0954-3899/39/7/075001.
2. P. Agostini et al., The Large Hadron–Electron Collider at the HL-LHC, *J. Phys. G* **48** (11), 110501 (2021). doi: 10.1088/1361-6471/abf3ba.
3. A. Abada et al., FCC-hh: The Hadron Collider: Future Circular Collider Conceptual Design Report Volume 3, *Eur. Phys. J. ST* **228** (4), 755–1107 (2019). doi: 10.1140/epjst/e2019-900087-0.
4. O. Brüning, LHeC Cost Estimate, *CERN-ACC-2018-0061* (2018).
5. S. A. Bogacz et al., Novel Lattices Solutions for the LHeC, *ICFA Beam Dynamics Newsletter* **71**, 135 (2017).
6. D. Pellegrini, A. Latina, D. Schulte, and S. A. Bogacz, Beam-dynamics driven design of the LHeC energy-recovery linac, *Phys. Rev. ST Accel. Beams* **18** (12), 121004 (2015). doi: 10.1103/PhysRevSTAB.18.121004.
7. G. H. Hoffstaetter and I. V. Bazarov, Beam-breakup instability theory for energy recovery linacs, *Phys. Rev. ST Accel. Beams* **7**, 054401 (2004). doi: 10.1103/PhysRevSTAB.7.054401.
8. A. Freiburger. 12 GeV CEBAF Upgrade, Reference Design: [www.jlab.org/physics/GeV/accelerator](http://www.jlab.org/physics/GeV/accelerator) (2012).
9. J. S. Schwinger, On radiation by electrons in a betatron, *Phys. Rev.* **70**, 798 (1946). doi: 10.2172/1195620.
10. K. D. J. André, Lattice Design and Beam Optics for the Energy Recovery Linac of the Large Hadron-Electron Collider, *Ph.D. Thesis, university Liverpool, UK* (in: prep).
11. I. Bejar Alonso et al., High Luminosity Hadron Collider, HL-LHC, technical design report, *CERN Yellow Report* **CERN 2020-10** (2020).
12. D. Angal-Kalinin et al., PERLE - Powerful energy recovery linac for experiments. Conceptual design report, *Journal of Physics G: Nuclear and Particle Physics* **45** (2018). ISSN 13616471. doi: 10.1088/1361-6471/aaa171.
13. C. Adolphsen et al., European Strategy for Particle Physics – Accelerator R&D Roadmap, *CERN Yellow Rep. Monogr.* **1**, 1–270 (2022). doi: 10.23731/CYRM-2022-001.